

Orbital Insulators and Orbital Order-disorder Induced Metal-Insulator Transition in Transition-Metal Oxides

Dong-Meng Chen^{1,2} and Liang-Jian Zou¹

*1 Key Laboratory of Materials Physics,
Institute of Solid State Physics, Chinese Academy of Sciences,
P. O. Box 1129, Hefei 230031, China and
2 Graduate School of the Chinese Academy of Sciences*

(Dated: May 23, 2019)

Abstract

The role of orbital ordering on metal-insulator transition of transition-metal oxides is investigated by the cluster self-consistent field approach in the strong correlation regime. A clear dependence of the insulating gap on the orbital order parameter is found in the single-particle excitation spectra. The thermal fluctuation drives the orbital order-disorder transition, diminishes the gap and leads to the metal-insulator transition. The interplay between spins and orbits results in unusual temperature dependence of the orbital polarization in the orbital insulator, which can be seen in the resonant x-ray scattering intensity.

PACS numbers: 71.30.+h, 75.40.Cx, 75.25.+z

I. INTRODUCTION

Metal-insulator transition (MIT) in strongly correlated transition-metal oxides (TMO) is one of the central problems in condensed matter physics, it has attracted extensive attention in recent decades since high temperature superconductivity and colossal magnetoresistance phenomena occur in the vicinity of MIT [1,2]. These strongly correlated electronic systems exhibit very complicated and rich phase diagrams with temperature, doping, pressure and magnetic field [3,4]. Of these, the temperature induced MIT in V_2O_3 and manganites is especially interesting, because the MIT temperature T_M is much smaller than the insulating gap (Δ) in transport, for example in V_2O_3 , $T_M=154$ K $\ll \Delta = 0.6$ eV [5]. Obviously, the thermal fluctuation is not the driven force of the MIT. It was recently realized that the orbital degree of freedom and orbital ordering (OO) play an important role on the ground state (GS) properties in these TMO.

The OO of 3d electrons was first proposed by Kugel et al. [6] for $KCuF_3$ and by Castellani et al. [7] for V_2O_3 to explain the complicated magnetic structures in these compounds. Due to the strong correlation between 3d electrons and large anisotropy of the 3d wavefunctions, the orbital degree of freedom and the OO have an important impact on the GS electronic and magnetic properties of these strongly correlated oxides [4, 6-9], and have been extensively studied in literatures in colossal magnetoresistive manganites, vanadium oxides and many other TMO (for example, see Ref.10). Experimentally orbital order-disorder transition is usually accompanied by MIT, OO transition (OOT) occurs almost at the critical point of the MIT, for example, in prototype Mott insulator V_2O_3 , an obvious insulator to metal transition occurs at $T_M=T_N$ [11], here T_N is the Curie-Weiss temperature. It is believed that in V_2O_3 , the OOT, the MIT and the magnetic transition occur simultaneously, or $T_M = T_{OO} = T_N$ [12]. We also notice that the ferromagnetic insulator to ferromagnetic metal transition at $T_{OO}(<T_N)$ in lightly doped $La_{0.88}Sr_{0.12}MnO_3$ is identified as an OOT at T_{OO} by Endoh *et al* [13], ruling out the significant role of cooperative Jahn-Teller (JT) distortion on the GS. This kind of orbital transition near the vicinity of MIT is also reported for $La_{1-x}Ca_xMnO_3$ near $x \approx 0.2$ [14]. These experiments clearly establish a close relationship between OOT and MIT. The possible correlation between OOT and MIT was first suggested by Castellani et al. [7] for V_2O_3 , they proposed that the MIT associated with the OO was driven by the variation of the entropy in the presence of the magnetic and orbital long range orders. Khaliulin et

al. [15] attributed this correlation to the formation of orbital polaron. Nevertheless, it is not well understood theoretically how the OOT and the MIT interplay with each other.

In this paper, we demonstrate that the strong orbital correlation of the partially filled 3d electrons in TMO leads to the GS as an orbital insulator. Starting from a twofold-degenerate spin-orbit interaction model, we studied the orbital order-disorder driven MIT using the cluster self-consistent field (cluster-SCF) approach developed recently. We showed that the insulating gap of the TMO opens as the orbital long-range order establishes. With increasing temperature the thermal fluctuation drives OOT in TMO, the resonant X-ray scattering (RXS) intensity diminishes to zero near the critical temperature T_{OO} , the energy gap of the single particle excitation also vanishes, indicating the insulator to metal transition. The rest of this paper is organized as follows: in Sec.II we describe the effective model Hamiltonian of an ideal orbital insulator and the cluster-SCF approach; then present the magnetic and orbital structures in GS, the T-dependent OO parameters and the single particle excitation spectra in Sec.III; the orbital polarization and azimuthal angle dependence of the RSX intensity is given in Sec.IV, and the last section is devoted to the discussion and summary.

II. MODEL HAMILTONIAN AND METHOD

In perovskite transition-metal oxides the fivefold degenerate 3d orbits of the transition metal ions splits into lower t_{2g} and higher E_g orbits under the octahedral crystalline field. For clarify and simplify we consider such an ideal cubic TMO system that t_{2g} orbits are filled and contribute no spin, and one hole or one electron occupies twofold degenerate E_g orbits, corresponding to the electron configuration of $3d^9$ or $3d^7$. Perovskite compounds KCuF_3 and LaNiO_3 are the possible candidates. The system is spin-1/2 and orbital twofold degenerate, denoting the orbital pseudospin $\tau=1/2$. Denotes the two E_g orbits as: $|1\rangle=|e_{g1}\rangle=|d_{3z^2-\tau^2}\rangle$, $|2\rangle=|e_{g2}\rangle=|d_{x^2-y^2}\rangle$. The low-energy physics of the system can be described by the twofold-degenerate Hubbard model with strong Coulomb interaction [6,7]. In the second-order perturbation approximation the E_g electrons interact with each other through the superexchange coupling, the low-energy effective Hamiltonian is expressed:

$$\hat{H}_{SE} = \sum_{\substack{\langle ij \rangle_l \\ l=x,y,z}} (J_1 \vec{s}_i \vec{s}_{j_l} + J_2 I_i^l \vec{s}_i \vec{s}_{j_l} + J_3 I_i^l I_{j_l}^l \vec{s}_i \vec{s}_{j_l} + J_4 I_i^l I_{j_l}^l) \quad (1)$$

where the operator $I_i^l = \cos(2\pi m_l/3)\tau_i^z - \sin(2\pi m_l/3)\tau_i^x$, the index l denotes the direction of a bond, $l = x, y$ or z , $\langle ij \rangle_l$ connects site i and its nearest-neighbor site j along the l direction, $(m_x, m_y, m_z) = (1, 2, 3)$. The orbital pseudospin operators τ_i^z and τ_i^x are the Pauli matrix, $\tau_i^z = \frac{1}{2}$ represents the orbital full polarization in $|1\rangle$ and $\tau_i^z = -\frac{1}{2}$ the orbital polarization in $|2\rangle$. Thus the polarization degree of the orbits is represented by $\langle \tau_i \rangle$, we call it the orbitalization. The constants J_1, J_2, J_3 and J_4 are the superexchange interactions and read: $J_1 = 8t^2 [U/(U^2 - J_H^2) - J_H/(U_1^2 - J_H^2)]$, $J_2 = 16t^2 [1/(U_1 + J_H) + 1/(U + J_H)]$, $J_3 = 32t^2 [U_1/(U_1^2 - J_H^2) - J_H/(U^2 - J_H^2)]$, and $J_4 = 8t^2 [(U_1 + 2J_H)/(U_1^2 - J_H^2) + J_H/(U^2 - J_H^2)]$, with $U = U_1 + 2J_H$, here $4t$ is the hopping integral of the E_g electrons along the z direction, U and U_1 are the intra- and inter-orbital Coulomb interactions, and J_H is the Hund's rule coupling, we adopt $t = 0.1$ eV and $J_H = 1.0$ eV.

It is still a difficult task to treat the correlation and fluctuation and to determine the GS of such strongly correlated systems in Eq.(1) with high accuracy. To study the GS properties of these TMO systems, we recently developed the cluster self-consistent field (cluster-SCF) approach to study the OO properties and the evolution of GS properties with interaction parameters in V_2O_3 [16]. This approach combines the exact diagonalization and the self-consistent field approaches, the main idea is briefly addressed as follows: first, we choose a proper cluster, usually the unit cell of the TMO compound, the electronic interactions of the cluster compose of two types: the internal bond interactions, H_{ij} , between the sites R_i and R_j in the cluster and the external bond interactions, H'_{il} , between the environment site R_l and the site R_i in the cluster. The periodic condition enforces the electronic states at environmental site R_l identical to the corresponding atom inside the cluster. After diagonalizing the internal interaction H_{ij} of the cluster, the interactions of the environment site R_l in H'_{il} acting on the cluster are obtained as a initial value of the self-consistent field (SCF): $H'_i = Tr_l(\rho_{il}H'_{il})$, here ρ_{il} is the reduced density matrix of the bond $\langle il \rangle$ after tracing over all of the other sites in the cluster. And then the cluster Hamiltonian H_{ij} is diagonalized in the presence of the SCF H'_i , iteration is then performed until the SCF H'_i converges. The GS properties and the effective field of the surrounding atoms applied on the inside atoms of the cluster are thus obtained. One of the advantages of the present approach is that the short-range correlation of spins and orbits, which is neglected in the conventional self-consistent mean field method, is taken into account.

III. ORBITAL TRANSITION INDUCED METAL-INSULATOR TRANSITION

In this section we first utilize the cluster-SCF method to find the magnetic and orbital GS of Eq.(1), then explore the evolution of OO phase with increasing temperature and the energy gap of single particle excitation spectra in the strong correlation limit.

A. Magnetic and orbital structures in ground state

In many three-dimensional TMO the magnetic structure is not difficult to determine by the neutron scattering and other experimental techniques, in the following we treat the large local spins as semiclassical to save computation time, and focus on the orbital fluctuation and the orbital GS for various magnetic orders. To determine the most stable magnetic and orbital GS structures of Eq.(1), we choose a pseudocubic 8-site cluster, an unit cell usually observed in many perovskite TMO. In the cluster, each site has three internal bonds and three external bonds. The total energy of the cluster as a function of the ratio U/J_H is

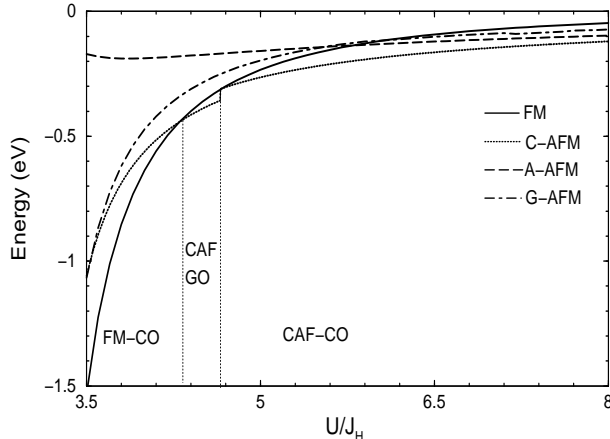


FIG. 1: Dependence of the total energy on the ratio U/J_H for different magnetic structures. FO, CAFO and GAFO denote the ferro-orbital, C-type, and *Neel* antiferro-orbital ordered structures, respectively. Theoretical parameters: $J_H = 1.0eV$ and $t = 0.1eV$.

calculated by the cluster-SCF method for various magnetic structures and is shown in Fig.1. It is found that for small U/J_H the GS is ferromagnetic (FM), which agrees with Roth [17] and Cyrot and Lyon-Caen's [18] mean field result, while the GS is C-type antiferromagnetic (C-type AFM or C-AFM) for large U/J_H , i.e. FM coupling along the c -axis and AFM

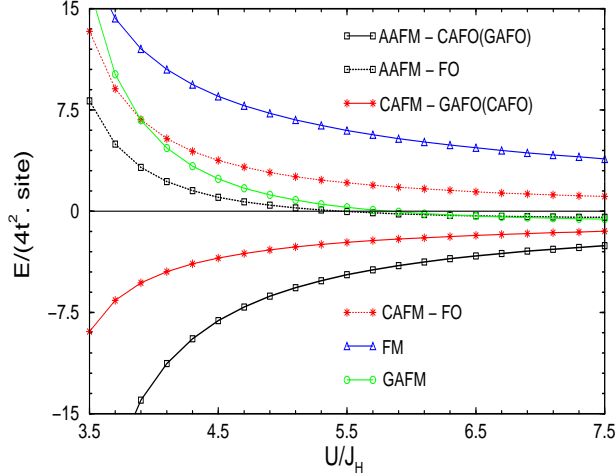


FIG. 2: GS energy dependence on the ratio U/J_H in the classical approximation. A-AFO denotes the A-type antiferro-orbital ordered structure. Theoretical parameters are the same to Fig.1

couplings in the ab -plane. As a contrast, the classical result shows that the spin coupling is AFM along the c -axis, and FM in the ab plane, the classical GS is A-type AFM structure (A-AFM) over very wide large U/J_H range, as seen in Fig.2. This classical result is in agreement with Kugel and Khomskii's result [6]. Obviously, the quantum fluctuation and the short-range correlation of the orbital pseudospins τ_i play essential roles on the GS orbital and spin configurations, leading the present GS to be significantly different from the classical result. The corresponding orbital configuration will be addressed more detail in terms of the orbital correlation functions later.

Large and small U/J_H favor different magnetic ordered GS, this can be seen from the dependence of the single-bond coupling energy on U/J_H in Fig.3. The single-bond coupling energy, which is calculated for different spin configurations via $E_{ij} = Tr(\rho_{ij} H_{ij})$, consists of the orbital-dependent spin coupling energy, as shown in Fig.3a, and the pure orbital coupling energy, as shown in Fig.3b. Due to the large hopping integral between two $|1\rangle$ orbitals along the z -axis, the z -bond energy proportional to $-4t^2/(U_1 - J_H)$ contributes dominantly to the GS energy, the corresponding spin alignment is FM and the orbital coupling is antiferro-orbital (AFO) over the whole U/J_H range, see Fig.3a and Fig.3b. Therefore the FM structure and the C-AFM structure with FM z -bond are the two candidates for the GS among all of the spin configurations. In contrast to the FM alignment in the z -axis, the spin arrangements along the x - and the y -axis are more easily changed. When U/J_H increases the magnetic

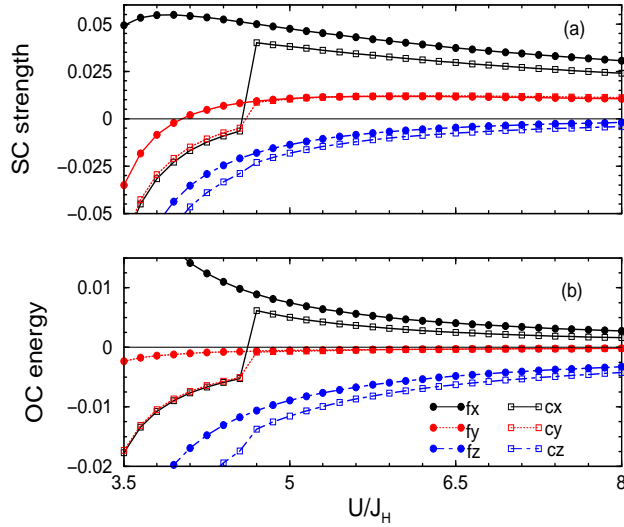


FIG. 3: Single-bond spin coupling strength (3a) and orbital coupling energy (3b) as the function of U/J_H for FM and C-AFM structures. $f_x(y,z)$ and $c_x(y,z)$ denote the bonds of FM and C-AFM structures along $x(y, z)$ directions, respectively.

transition from FM to C-AFM structures is found at $(U/J_H)_c \approx 4.3$, which can be seen clearly in Fig.1. This quantum magnetic transition is also shown in Fig.3b. For small U/J_H , the quantum fluctuation of spins is small, so the FM structure is the most stable; On the contrary, the C-AFM structure is more stable for large U/J_H . In Fig.3a the single-bond spin coupling along the x-axis in the FM structure is not negative, this arises from the frustration effect of the spin and orbital correlation in quarter-filling TMO with cubic lattice: in the FM phase, the effective Hamiltonian (1) reduces to $\sum_{\langle ij \rangle_l} \tau_i^l \tau_j^l$ and $\sum_i \tau_i^z$. Obviously the second term arising from the orbital anisotropy as shown in Ref.[9] favors the orbital occupation along the z-axis, leading to strong quantum fluctuation of the orbital pseudospins along the x-axis. Another origin of the frustration comes from the off-diagonal hopping between transition-metal ions when the long range OO establishes. And we notice that the pure orbital coupling contributes more to the single bond energy than the orbital-dependent spin coupling.

To determine the GS orbital configuration, we studied the nearest-neighbor orbital correlation function: $C_{ij} = \langle \vec{\tau}_i \cdot \vec{\tau}_j \rangle - \langle \vec{\tau}_i \rangle \cdot \langle \vec{\tau}_j \rangle$, and the orbital polarization $\langle \vec{\tau} \rangle$ for the FM and C-AFM structures in different U/J_H ranges. In the FM GS regime ($U/J_H < 4.3$), we find each site is strongly AFO polarized with respect to its nearest-neighbor sites in the $y-z$ plane

and weakly ferro-orbital (FO) polarized along the x axis, indicating that the orbital structure is C-type AFO (C-AFO) ordered phase. The orbital occupations in the two sublattices are the combinations of $|1\rangle$ and $|2\rangle$, which is $(|1\rangle + \sqrt{15}|2\rangle)/4$, and $(\sqrt{55}|1\rangle - \sqrt{3}|2\rangle)/8$ orbits at $U/J_H=4.0$. This orbital configuration is slightly different from Cyrot and Lyon-Caen's *Neel* AFO result and Roth's FO result.

In the present cubic FM structure, one would anticipate that all of the orbital correlation of the three bonds are AFO, as expected in Kanamori-Goodenough empirical rule [19]. However the weak FO correlation along the x -axis indicates that there exists frustration effect in the cubic spin-orbit interaction systems, this also agrees with the weak positive single-bond spin coupling strength along the x -axis in the FM GS. This also shows that the importance of the cluster SCF method in concerning the short-range orbital correlations. For large U/J_H , when the Coulomb interaction U is sufficiently large ($U/J_H > 4.6$), the GS orbital configuration is the C'-type AFO (C'-AFO) ordered phase, i.e. AFO coupling in the $y - z$ plane and FO coupling along the x axis, but with the correlation strengths different from the FM structure. The abrupt change of the GS energy at $U/J_H = 4.6$ is associated with the orbital phase transition from G-type AFO to C'-AFO structures. We further find that there exists a crossover regime ($4.3 < U/J_H < 4.6$) in which the FM and C-type AFM structures compete with each other, and lead to the G-type AFO ordered phase as the GS. Therefore in the present cluster-SCF method, the degeneracy of the G-AFO and the C'-AFO configuration is lifted, different from Kugel and Khomoski's degenerate result [6].

It is more interested that in such a strongly correlated orbital system, the entanglement of the orbital states is associated with the quantum phase transition, we find that the concurrence of the nearest-neighbor two pseudospins critically changes at the quantum transition point, detail result will be published in the future. On the other hand, if we freeze the orbital configuration as the C-AFO ordered phase to study the most stable spin configurations, we find that the magnetic structure transition from FM to C-AFM also occurs at the same critical value $(U/J_H)_c=4.3$.

B. Temperature Dependence of Orbital Order Parameter

After determining the ordered orbital phase in the GS, we explore the influence of the thermal fluctuation on the spin and orbital order parameters. At finite temperature T ,

thermal fluctuation exciting spin wave and orbital wave weakens both the orbital and the spin long-range orders, and destroys the magnetic order at the critical temperature T_N and the OO at the critical temperature T_{OO} . Since the spin order interplays with the OO, the reduction of spontaneous magnetization with increasing temperature also softens the orbital interaction, and *vice versa*. In the following we study the temperature dependence of the spin order and the OO parameters at small $U/J_H < 4.3$ in the self-consistent mean field approximation. The effective Hamiltonian H_{SE} is then approximated as:

$$H_{MF} = \sum_i (J_{A(B)z} \tau_{iA(B)}^z + J_{A(B)x} \tau_{iA(B)}^x + J_s s_i^z) \quad (2)$$

where the coefficients $J_{A(B)z}$, $J_{A(B)x}$ and J_s depend on the spin order and the OO parameters, for example:

$$J_s = [-6J_1 + J_3 (\langle I_A^x \rangle \langle I_A^x \rangle + \langle I_B^x \rangle \langle I_B^x \rangle + 2 \langle I_A^y \rangle \langle I_A^y \rangle + 2 \langle I_A^z \rangle \langle I_A^z \rangle)] \langle s^z \rangle \quad (3)$$

etc. In the GS with FM and C-AFO orders, the thermal averages of the spontaneous magnetization and the orbital polarization, i.e. the orbitalization, satisfy the following self-consistent equations:

$$\langle s_a^z \rangle = Tr \{ s_a^z \exp(-\beta J_{sa} s_a^z) \} / Z_a^s \quad (4)$$

$$\langle \tau_A^{x(z)} \rangle = Tr \{ \tau_A^{x(z)} \exp(-\beta J_A^{x(z)} \tau_A^{x(z)}) \} / Z_A^{x(z)} \quad (5)$$

where $\beta = -1/k_B T$. The self-consistent mean-field equations for the C-AFM and C'-AFO phase can be obtained, but are more complicated. The temperature dependence of the spin and OO parameters for the system with small U/J_H is shown in Fig.4. At low temperature, the magnetization and the two components of the orbitalization are nearly saturated. At lifting temperature $T > T_M/2$, the spin order parameter, magnetization, begins to considerably decrease, while the orbitalization $\langle \tau \rangle$ still keeps saturation. With the temperature approaching T_N , the magnetization rapidly falls to zero, the magnetic transition is obviously the first order, which originates from the strong anisotropy of the spin-orbit coupling, in agreement with Rice's argument based the Landau phenomenal theory for multiple parameter orders, and our renormalization group analysis to the critical indexes of the effective Hamiltonian also confirmed this point; meanwhile the OO parameter steeply diminishes an increment, as seen in Fig.4. With further increasing temperature, the OO parameter gradually decreases and finally vanishes at $T = T_{OO}$, with the characters of the second-order phase transition.

Due to then highly anisotropy and lower symmetry than $SU(4)$ in the spin-orbit coupling, the long-range orbital-orbital correlation still exists even if the magnetic order disappears, therefore the orbital order-disorder transition temperature T_{OO} is higher than the magnetic transition temperature T_N , as observed in Fig.4. It is of worthwhile noticing that the orbitalization components $\langle \tau^z \rangle$ and $\langle \tau^x \rangle$ displaying considerable discontinuity at the Curie-Weiss temperature T_N indicates the strong correlation between the spin and the orbital degrees of freedom, the RXS intensity also exhibits the discontinuity, as we will show in Sec.IV.

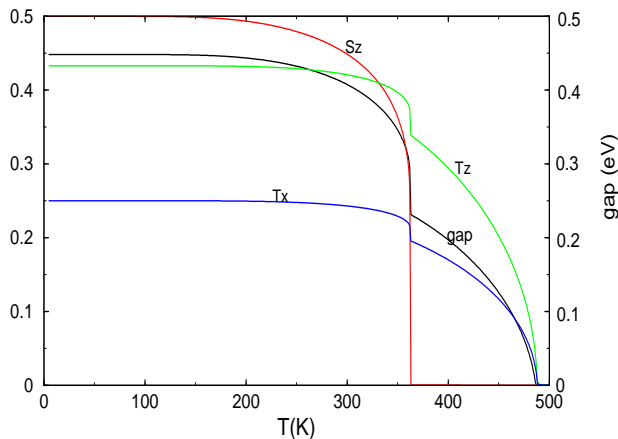


FIG. 4: Temperature dependence of the magnetization s_z , the orbital polarization τ_z and τ_x , and the energy gap. Theoretical parameters: $U = 4.0eV$, $U_1 = 2.0eV$, $J_H = 1.0eV$, $t = 0.1eV$ and $\lambda = -0.1eV$.

C. Energy gap of single particle spectra

In the following we study how the single particle energy spectra of the E_g electrons depends on the OO parameter. In the OO phase, the orbital long-range order breaks the symmetry of the system in orbital space, and opens an insulating gap Δ in single-particle excitation spectra of the TMO. Such an orbital insulator differs from single-band Mott-Hubbard insulators in many aspects. One of the outstanding characters is that the insulating gap closely depends the OO parameter, hence the temperature. In the OO TMO at quarter filling when a small fraction of holes are introduced into the orbital insulating TMO, the

tight-bonding spectrum of an E_g hole reads:

$$H_t = t \sum_{\langle i,j \rangle_{x,y}} \left[d_{i1}^\dagger d_{j1} \pm \sqrt{3} \left(d_{i1}^\dagger d_{j2} + d_{i2}^\dagger d_{j1} \right) + 3d_{i2}^\dagger d_{j2} \right] + 4t \sum_{\langle i,j \rangle_z} d_{i1}^\dagger d_{j1} + H.C. \quad (6)$$

where $d_{i\gamma}^\dagger$ creates a 3d electron at site i with orbital state γ , and \pm denote the signs of the hopping integrals between two nearest-neighbor sites along the x and y direction, respectively.

Strong on-site Coulomb interaction U is the main character in these ordered TMO, that $U \gg t$ prohibits the E_g electrons from double occupation at the same site, the single occupation constraint is thus applied on the E_g orbits. In the limit of large Coulomb interaction, the constraint of no double occupancy at site R_i is enforced by introducing auxiliary fermions [20], $f_{i\gamma}^\dagger$, and bosons, b_i , where $f_{i\gamma}^\dagger$ creates a slaved fermion (electron) at site R_i with orbital state γ , and b_i^\dagger creates a boson (hole) at site R_i , thus $d_{i\gamma\sigma}^\dagger = f_{i\gamma\sigma}^\dagger b_i$, and the single occupation condition is: $\sum_{\sigma\gamma} f_{i\gamma\sigma}^\dagger f_{i\gamma\sigma} + b_i^\dagger b_i = 1$. In the FM and C-AFO ordered structure, the mean-field Hamiltonian becomes:

$$H_{MF} = \sum_k [\epsilon_k^{11} f_{k1}^\dagger f_{k1} + \epsilon_k^{22} f_{k2}^\dagger f_{k2} + \epsilon_k^{12} (f_{k1}^\dagger f_{k2} + f_{k2}^\dagger f_{k1}) + \tilde{J}_1 (f_{k+Q,1}^\dagger f_{k1} - f_{k+Q,2}^\dagger f_{k2}) + \tilde{J}_2 (f_{k+Q,2}^\dagger f_{k1} + f_{k+Q,1}^\dagger f_{k2})] + \sum_k \lambda (f_{k1}^\dagger f_{k1} + f_{k2}^\dagger f_{k2} + x - 1) \quad (7)$$

with $Q = (0, \pi, \pi)$ corresponding to the C-AFO ordering, the parameters \tilde{J}_1 and \tilde{J}_2 are: $\tilde{J}_1 = (J_3 \langle s^z \rangle^2 + J_4) (\sqrt{3} \langle \tau^x \rangle - 2 \langle \tau^z \rangle)$, $\tilde{J}_2 = \sqrt{3} (J_3 \langle s^z \rangle^2 + J_4) \langle \tau^x \rangle$, respectively; the dispersion functions are: $\epsilon_k^{11} = 4xt (\cos k_x + \cos k_y + 4 \cos k_z)$, $\epsilon_k^{12} = 4\sqrt{3}xt (-\cos k_x + \cos k_y)$, $\epsilon_k^{22} = 12xt (\cos k_x + \cos k_y)$; and the hole concentration $\langle b_i^\dagger b_i \rangle \ll 1$. In the saddle-point approximation, the constraint constant λ and the boson occupation are:

$$\lambda = -\frac{1}{N} \sum_{\langle i,j \rangle \gamma \gamma'} \left(t_{ij}^{\gamma \gamma'} \langle f_{i\gamma}^\dagger f_{j\gamma'} \rangle + H \cdot C \right) \quad (8)$$

$$x = 1 - \frac{1}{N} \sum_i \left(\langle f_{i1}^\dagger f_{i1} \rangle + \langle f_{i2}^\dagger f_{i2} \rangle \right) \quad (9)$$

Physically λ shifts the energy level of the fermi quasiparticles, and x gives rise to the hole concentration. The single quasiparticle energy spectra ω_k have four branches and strongly depend on the OO parameter. For the C-AFO ordered TMO the lower two subbands are filled, the minimum of the empty subband separates from the maximum of the filled subband by a gap Δ . This result considerably differs from Kilian and Khaliulian's gapless charge

excitation [15]; in fact, they did not taken into account the modification of the presence of orbital order to the motion of the electrons.

The thermal fluctuation softens the OO parameter, hence softening the single-particle excitation spectra. The energy spectra at different temperatures are shown in Fig.5. At

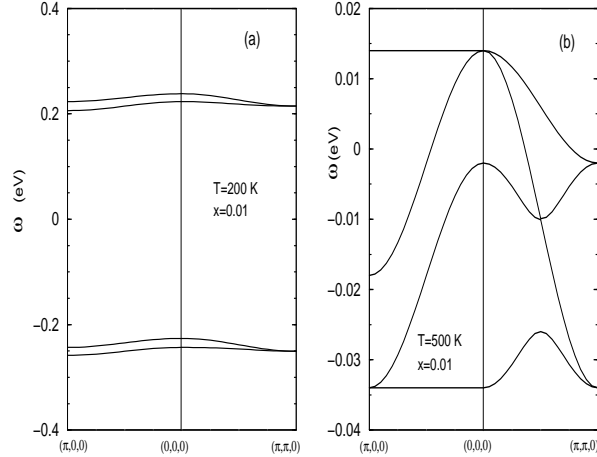


FIG. 5: The energy spectra at $T < T_{OO}$ (a) and $T > T_{OO}$ (b) in the ferromagnetic and C-type antiferro-orbital ordered state. Parameters are the same to Fig.4.

low T , the strong Coulomb interaction of the 3d electrons and the large spatial anisotropy of 3d orbits lifts the orbital degeneracy, and favors ordered orbital phase. The broken of the orbital space symmetry leads to that an electron must cost at least Δ in energy to hop to the nearest-neighbor site, therefore the threshold Δ gives rise to the insulating gap of the quarter-filling TMO as an orbital insulator. In this situation the two lower subbands are occupied and another two higher subbands are empty with separation Δ (see Fig.5a). Doping and increasing temperature gradually destroy the orbital long-range order, and lead to the merge of the separated subbands. With the increasing of temperature to $T > T_{OO}$, the thermal fluctuation becomes so strong that the long-range OO is destroyed, and the OO parameter vanishes; the two lower subbands merge with two higher subbands together, the insulating gap disappears (see Fig.5b), indicating the occurrence of MIT in TMO. Thus the energy gap of the orbital insulator crucially depends on the OO parameter. The temperature dependence of the insulating gap $\Delta(T)$ turns out to be similar to that of the OO parameter, which diminishes steeply at the Curie-Weiss temperature T_N and completely disappears at T_{OO} . Therefore, the temperature driven MIT in TMO is essentially induced by the orbital order-disorder transition.

IV. RESONANT X-RAY SCATTERING INTENSITY OF ORBITAL INSULATOR

The optical excitation of orbital insulating TMO also demonstrates the strong coupling between spins and orbits. The polarization and azimuthal dependences of the RXS intensity provide hidden information of the underlying OO parameters [21-24], and unveil the interplay between spins and orbits. Utilizing the RXS technique to measure the OO phase in TMO was proposed recently by Murakami et al. [22] for manganites and Fabrizio et al. [23] for V_2O_3 . The $1s - 3d$ K-edge RXS peak intensity is a powerful signal to probe the OO phase and the orbital order-disorder phase transitions [11,21]. Although the signal enhancement of the quadrupolar $1s - 3d$ scattering (E_2) is less than that of the electric dipole $1s - 4p$ scattering (E_1), the observed E_2 spectral line shape as a function of energy is more easy to identify than the quite complicated line shapes associated with E_1 process [11,22,23]. In the following we present the E_2 RXS intensity based on the OO states obtained in the preceding section.

In the FM and C-AFO ordered GS, the ordered 3d orbital states consist of two different orbits: $|\psi_1\rangle = \alpha_1 |1\rangle + \alpha_2 |2\rangle$ and $|\psi_2\rangle = \beta_1 |1\rangle + \beta_2 |2\rangle$, here the coefficients $\alpha_{1,2}$ are the functions of the interaction parameters. There exist two kinds of reflections: the fundamental reflection at $(hkl) = (n_x n_y n_z)$ and the orbital superlattice reflection at $(hkl) = (n_x, n_y + \frac{1}{2}, n_z + \frac{1}{2})$. At lattice symmetry-forbidden (hkl) satisfying $h + k + l = 2n + 1$, n is an integer, the orbital structure factor is written as:

$$F_{hkl} = f(\Gamma, r_{2,ds}, c, \omega) \sqrt{n_{\epsilon k} n_{\epsilon' k'}} \{ \langle \tau_z \rangle [(\epsilon'_x k'_x - \epsilon'_y k'_y) (\epsilon_x k_x - \epsilon_y k_y) - 3\epsilon'_z k'_z \epsilon_z k_z] + 2\sqrt{3} \langle \tau_x \rangle [\epsilon_z k_z (\epsilon'_x k'_x - \epsilon'_y k'_y) + (\epsilon_x k_x - \epsilon_y k_y) \epsilon'_z k'_z] \} \quad (10)$$

where the function $f(\Gamma, r_{2,ds}, c, \omega)$ is the coefficient depending on the lifetime of the intermediate states, Γ , the radial matrix element $r_{2,ds}$, the velocity of photon c and the incoming photon frequency ω ; $n_{\epsilon(\epsilon'), k(k')}$ is the density of the incoming(outgoing) beam of photons with polarization $\vec{\epsilon}(\vec{\epsilon}')$ and wavevector $\vec{k}(\vec{k}')$. When the incoming beam is a perfect σ -polarization, the orbital structure factors for unrotated ($\sigma\sigma'$) and rotated ($\sigma\pi'$) channels are:

$$F_{\sigma\sigma'} = f(\Gamma, r_{2,ds}, c, \omega) \sqrt{n_{\epsilon k} n_{\epsilon' k'}} \langle \tau_z \rangle \cos^2 \theta \sin^2 2\varphi \quad (11)$$

$$F_{\sigma\pi'} = f(\Gamma, r_{2,ds}, c, \omega) \sqrt{n_{\epsilon k} n_{\epsilon' k'}} \left[-\frac{1}{4} \langle \tau_z \rangle \sin 4\varphi + \sqrt{3} \langle \tau_x \rangle \sin 2\varphi \right] \cos \theta \sin 2\theta$$

where θ and φ are the Bragg and the azimuthal angles, respectively. The temperature dependence of the intensities at a selected azimuthal of the OO superlattice Bragg reflection (003) are shown in Fig.6. A step decrease of the RXS intensities at T_N is observed in Fig.6,

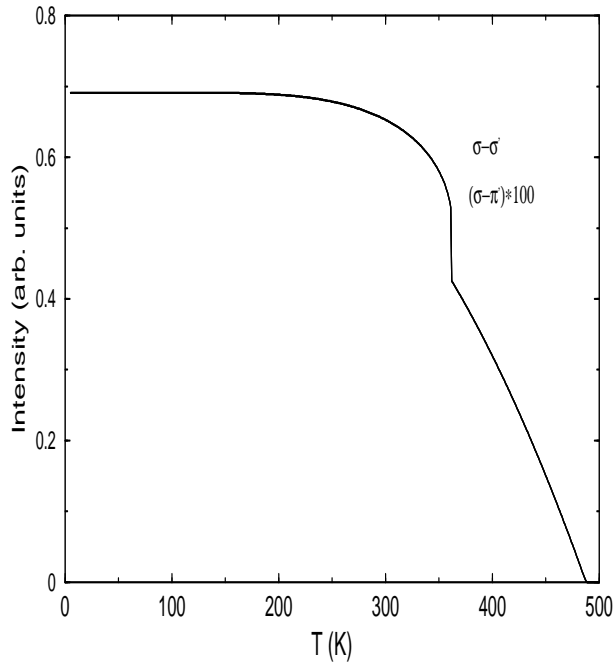


FIG. 6: Temperature dependence of RXS intensity of C-type orbital ordered phase in (003) direction for rotated ($\sigma\pi'$) and unrotated ($\sigma\pi$) channels.

this discontinuous decrease is associated with the lost of magnetic long-range order, which diminishes a fraction of orbital interaction. The K-edge RXS peaks disappear completely at the OO or MIT transition point, therefore the RXS intensity could be a probe to the critical point of MIT in orbital insulators. This discontinuous decrease is widely observed in the RXS experiments in manganites, KCuF_3 and YVO_3 , a significant evidence of the strong spin-orbit coupling.

V. REMARKS

In the preceding sections we focus on the FM and C-AFO structure. For large U/J_H , the GS is C-AFM and C'-AFO ordered phase as determined by the cluster-SCF approach, we also find such orbital ordered TMO opens an insulating gap in the single particle energy spectra, and the energy gap exhibits similar dependences on the OO parameter and the

temperature to those in the FM C-AFO ordered phase. The dependence of the RXS intensity on temperature is also the same as the preceding structure qualitatively, though the peak positions of the RXS intensity slightly shift in comparison with the preceding structure. Therefore different ordered orbital insulators share many common characteristics, which are significantly different from the conventional single-band Mott-Hubbard insulators [1, 25].

Many cubic symmetric TMO with orbital degeneracy are inherently unstable, the orbital degeneracy is usually lifted by lowering the crystal symmetry through the Jahn-Teller distortion in LaMnO_3 and YVO_3 or other lattice distortion modes in V_2O_3 . As far as the static Jahn-Teller effect is considered, the GS orbital configuration is modified by the following orbital coupling [9]:

$$\hat{H}_{JT} = \sum_{\langle ij \rangle}^{x,y,z} \frac{2g^2}{3K} I_i^l I_j^l \quad (12)$$

where g is the electron-phonon coupling constant, and K the restoring coefficient. For typical TMO in which Jahn-Teller effect plays a role, the parameters $g \sim 1.2$ eV, and $K \sim 10.0$ eV. In these systems, the spin-orbit coupling arises from both the Coulomb interaction and the Jahn-Teller effect, thus the orbital GS is a combination of the pure electronic spin-orbital superexchange interaction described by Eq.(1) and the static Jahn-Teller orbital interaction by Eq.(12). Utilizing the cluster-SCF method, we find that the most stable GS magnetic structure of Eqs.(1) and (12) is the A-AFM order for large U/J_H , and the orbital polarization is G-AFO ordered; and for small U/J_H the GS is FM and C-AFO order. The system also exhibits most of these properties of orbital insulators. Detail results incorporated with the correction of the relativistic LS coupling [26] and the comparison with the OO in KCuF_3 will be published in the future paper.

An obvious fact is that many OO insulators do not exhibit MIT when the long-range OO disappears at high temperature, such as in LaMnO_3 [27], YVO_3 [28], etc., except for V_2O_3 . The essential reason is that these TMO are not simple orbital insulators, there also exists strong dynamic electron-phonon coupling, i.e., the dynamic Jahn-Teller effect, even if the static cooperative Jahn-Teller distortion disappears at high temperature. In these compounds, numerous dynamic Jahn-Teller phonons surround the 3d electrons, localize the 3d electrons as incoherent polarons. The transport of the 3d electrons is dragged by dynamic phonons, the electronic transport is of insulated polaronic character. Therefore these TMO with the Jahn-Teller effect are still insulators at high temperature.

In summary, in a pure two-orbital degenerate electronic spin-orbit interacting TMO system, besides the orbital wave gap, an energy gap of the electron excitation is opened as the orbital order develops, and disappears with the vanish of the OO driven by the thermal fluctuation. A clear dependence of the insulating gap on the orbital order parameters shows that such TMO possesses the orbital insulator characters. The RXS intensity also exhibit the close interplay between spin and orbit orders. We expect more interesting properties of orbital insulator will be uncovered in the further studies.

Acknowledgments

Supports from the NSF of China and the BaiRen project from the Chinese Academy of Sciences (CAS) are appreciated.

-
- [1] M. Imada, A. Fujimori and Y. Tokura, *Rev. Mod. Phys* **70**, 1039 (1998).
- [2] S. Jin, T. H. Tiefel, M. McCormack, R. A. Fastnacht, R. Ramesh and L. H. Chien, *Science* **264**, 413 (1994).
- [3] I. Loa, P. Adler, A. Grzechnik, K. Syassen, U. Schwarz, M. Hanfland, G. K. Rozenberg, P. Gorodetsky and M. P. Pasternak, *Phys. Rev. Lett.* **87**, 125501 (2001).
- [4] For example, see Y. Tokura and N. Nagaosa, *Science*, **288**,462 (2000).
- [5] G. A. Thomas, D. H. Rapkine, S. A. Carter, A. J. Millis, T. F. Rosenbaum, P. Metcalf and J. M. Honig, *Phys. Rev. Lett.* **73**, 1529 (1994).
- [6] K. I. Kugel and D. I. Khomskii, *Sov. Phys. JETP* **37**, 725 (1973).
- [7] C. Castellani, C. R. Natoli and J. Ranninger, *Phys. Rev.* **B18**, 4945 (1978).
- [8] D. I. Khomskii, *J. Mod. Phys.* **B15**, 2665 (2001).
- [9] D. I. Khomskii and M.V. Mostovoy, *cond-mat/0304089*.
- [10] Y. Tokura and N. Nagaosa, *Science*, **288** 462 (2000).
- [11] D. B. Mcwhan, J. P. Remeika, T. M. Rice, W. F. Brinkman, J. P. Maita and A. Menth, *Phys. Rev. Lett.* **27**, 941 (1971); *Phys. Rev.* **B7**, 1920 (1973).
- [12] L. Paolasini, C. Vettier, F. de Bergevin, F. Yakhou, D. Mannix, A. Stunault, W. Neubeck, M. Altarelli, M. Fabrizio, P.A. Metcalf and J.M. Honig, *Phys. Rev. Lett.* **82**, 4719 (1999).
- [13] Y. Endoh , K. Hirota, S. Ishihara, S. Okamoto, Y. Murakami, A. Nishizawa, T. Fukuda, H. Kimura, H. Nojiri, K. Kaneko and S. Maekawa, *Phys. Rev. Lett.* **82**, 4328 (1999).
- [14] B. B. Van Aken, O. D. Jurchescu, A. Meetsma, Y. Tomioka and T.M. Palstra, *Phys. Rev. Lett.* **90**, 066403 (2003).
- [15] R. Kilian and G. Khaliullin, *Phys. Rev.* **B60**, 13458 (1999).
- [16] Liang-Jian Zou, M. Fabrizio and M. Alteralli, *Preprint*.
- [17] L. M. Roth, *Phys. Rev.* **146**, 306 (1966).
- [18] M. Cyrot and C. Lyon-Caen, *J. Phys. (Paris)* **36**, 253 (1975).
- [19] J. Kanamori *J. Phys. Chem. Solids* **10**, 87 (1959); J. B. Goodenough *Phys. Rev.* **100**, 564 (1955).
- [20] N. Read and D. M. Newsn, *Solid State Commun.* **52**, 993 (1984).
- [21] M. Altarelli, *Complementary between Neutron and Synchrotron X-Ray Scattering*, Ed. by A.

- Furrer, (World Scientific, 1998).
- [22] Y. Murakami, H. Kawada, H. Kawata, M. Tanaka, T. Arima, Y. Moritomo and Y. Tokura, *Phys. Rev. Lett.* **80**, 1932 (1998).
- [23] M. Fabrizio, M. Altarelli and M. Benfatlo, *Phys. Rev. Lett.* **80**, 3400 (1998); *Phys. Rev. Lett.* **81**, E4030 (1998).
- [24] S. Ishihara and S. Maekawa, *Phys. Rev.* **B58**, 13442 (1998).
- [25] N. F. Mott, *Metal-Insulator Transitions*, Taylor and Francis, London/Philadelphia, (1990).
- [26] N. Binggeli and M. Alteralli, *Phys. Rev.* **B70**, 085117 (2004).
- [27] J. Geck, P. Wochner, D. Bruns, B. Buchner, U. Gebhardt, S. Kiele, P. Reutler, and A. Revcolevschi, *Phys. Rev.* **B69**, 104413 (2004).
- [28] For example, see G. R. Blake, T. T.M. Palstra, Y. Ren, A. A. Nugroho and A. A. Mwnovsky, *Phys. Rev. Lett.* **87**, 245501 (2001).